Explanation of the barrier heights of graphene Schottky contacts by the MIGS-and-electronegativity concept

Winfried Mönch[a)]
Faculty of Physics, Universität Duisburg-Essen, 47048 Duisburg, Germany

(Received 15 June 2016; accepted 24 August 2016; published online 8 September 2016)

Graphene-semiconductor contacts exhibit rectifying properties and, in this respect, they behave in exactly the same way as a "conventional" metal-semiconductor or Schottky contacts. It will be demonstrated that, as often assumed, the Schottky-Mott rule does not describe the reported barrier heights of graphene-semiconductor contacts. With "conventional" Schottky contacts, the same conclusion was reached already in 1940. The physical reason is that the Schottky-Mott rule considers no interaction between the metal and the semiconductor. The barrier heights of "conventional" Schottky contacts were explained by the continuum of metal-induced gap states (MIGSs), where the differences of the metal and semiconductor electronegativities describe the size and the sign of the intrinsic electric-dipoles at the interfaces. It is demonstrated that the MIGS-and-electronegativity concept unambiguously also explains the experimentally observed barrier heights of graphene Schottky contacts. This conclusion includes also the barrier heights reported for MoS_2 Schottky contacts with "conventional" metals as well as with graphene. *Published by AIP Publishing.*
[http://dx.doi.org/10.1063/1.4962310]

I. INTRODUCTION

Graphene is a single layer of sp^2-bonded carbon atoms arranged in a hexagonal crystal lattice. The remaining $2p_z$ orbitals, which are perpendicular to the graphene plane, form π and π^* bands. They meet at the K points of the Brillouin zone,[1,2] so that graphene may be described either as a gapless semiconductor or a zero-overlap semimetal.[3]

Graphene (Gr) is a unique material that combines many superior properties. It is characterized, for example, by an extremely high room-temperature electron mobility, low optical absorption, high thermal conductivity, complete impermeability to gases, high Yong's modulus, and high intrinsic strength.[4] Furthermore, graphene can be chemically functionalized. In "*A roadmap for graphene*," Novoselov *et al.*[4] described and critically analyzed numerous potential applications. But already Geim and Novoselov[5] warned that some of the "graphene dreams" are unlikely to appear for the next 20 years.

In graphene-semiconductor devices, Gr-semiconductor junctions are the most basic components. As most of the "conventional" metal-semiconductor or Schottky contacts, they exhibit rectifying behavior. In the following, published experimental barrier heights of graphene Schottky contacts will be systematically analyzed and, as the barrier heights of the "conventional" Schottky contacts, they will be finally explained by the concept of metal-induced gap states (MIGSs).

II. SOME EXPERIMENTAL NOTES

The graphene Schottky contacts discussed in the following were fabricated by either micro-mechanical exfoliation of monolayer flakes from graphite crystals or by transfer of graphene layers grown by chemical vapor deposition (CVD) on non-carbide forming transition metal substrates (see, for example, Ref. 4 and references cited therein). On SiC substrates, graphene layers were also prepared by *in situ* desorption of silicon atoms at elevated temperatures (see, for example, Ref. 4 and references cited therein). This most elegant method, however, produces no intimate Gr-SiC contacts but is accompanied by intermediate "buffer layers."

The barrier heights of the Gr Schottky contacts discussed in the following were determined from their current-voltage (I/V) and capacitance-voltage (C/V) characteristics or by using X-ray photoemission spectroscopy (XPS) (see, for example, Ref. 6 and references cited therein). The I/V barrier heights and ideality factors generally vary from one contact to the next even if they were fabricated in the same way, and they strongly depend on temperature. This is caused by patches of reduced barrier height and lateral dimensions smaller than the depletion layer width which dominate the current transport.[7] However, a theoretical analysis of experimental data requires the barrier heights of laterally homogeneous Schottky contacts. They can be obtained from the temperature dependence of the effective I/V barrier heights by assuming a Gaussian distribution of the patch barrier heights[8] and from the linear correlation between the effective I/V barrier heights and the ideality factors.[9] The evaluation of C/V characteristics directly yields the flat-band barrier heights which equal the barrier heights of the laterally homogeneous contact (see, for example, Ref. 6). XPS also gives the barrier heights of the laterally homogeneous contacts as long as the patches of lowered barrier heights do not dominate (see, for example, Ref. 6).

III. SCHOTTKY-MOTT RULE

The attempts to explain the experimentally observed barrier heights of graphene Schottky contacts mostly applied the Schottky-Mott rule[10,11]

[a)]Electronic mail: winfried.moench@uni-due.de

$$\Phi_{Bn} = \Phi_m - \chi_s, \quad (1)$$

i.e., the n-type barrier height $\Phi_{Bn} = W_c - W_F$ is considered to equal the difference between the work function $\Phi_m = W_{vac} - W_F$ of the metal, in the present case graphene, and the electron affinity $\chi_s = W_{vac} - W_c$ of the semiconductor. Here, W_F is the Fermi level, W_{vac} is the vacuum level, and W_v and W_c are the valence-band maximum and the conduction-band minimum of the semiconductor, respectively. The semiconductors are assumed to be doped n-type. Figure 1 displays experimental barrier heights of laterally homogeneous graphene Schottky contacts[12–31] as a function of the barrier heights expected from the Schottky-Mott rule (1). The experimental work function of graphene amounts to 4.56 eV,[32,33] and the electron affinities of the semiconductors were calculated as the differences $\chi = I - W_g$ of the experimental ionization energies $I = W_{vac} - W_v$ and the band gaps $W_g = W_c - W_v$. The respective data are compiled in Table I. Obviously, the experimental barrier heights of the graphene Schottky contacts do not agree with the values predicted by the Schottky-Mott rule. For "conventional" metal-semiconductor contacts, Schottky[11] reached the same conclusion already in 1940.

The Schottky-Mott rule is the result of a *Gedanken* experiment where a metal and an ideal semiconductor with no surface states at all face each other in vacuum. The work functions of the two solids generally differ so that an electric field exists between them. The screening lengths of the electrons (holes) in n-type (p-type) semiconductors, the Debye lengths, are by many orders of magnitude larger than the Thomas-Fermi screening lengths of metals, because the electron densities of metals are much larger than the densities of mobile carriers in non-degenerately doped semiconductors. As the vacuum gap is reduced, the electric-field thus penetrates the semiconductor, i.e., a band bending builds up beneath the semiconductor surface. Supposed the work function of the metal is larger than the one of the n-type (p-type) semiconductors, the surface becomes depleted of electrons (holes) and the respective space charge is provided by the immobile and then uncompensated donors (acceptors). When the vacuum gap is eventually closed, i.e., in the limit of an "intimate" contact, the vacuum levels of the metal and the semiconductor will align. Hence, the Schottky-Mott barrier height equals the difference between the work function of the metal and the electron affinity (ionization energy $I = W_{vac} - W_v$) of the n-type (p-type) semiconductor.

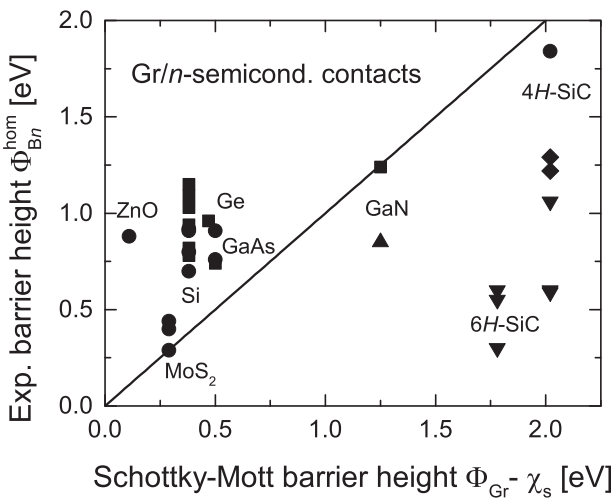

FIG. 1. Experimental barrier heights of laterally homogeneous Gr Schottky contacts as a function of the respective barrier heights predicted by the Schottky-Mott rule (1). Experimental data from Refs. 12–32. The contacts were fabricated by using exfoliated Gr flakes (●, ▲), transfer of CVD-grown Gr layers (■, ◆), and surface decomposition of SiC (▼).

TABLE I. Band-gaps $W_g = W_c - W_v$, ionization energies $I = W_{vac} - W_v$, electron affinities $\chi_s = I - W_g$, and branch-point energies $\Phi^p_{bp} = W_{bp} - W_v$ and $\Phi^n_{bp} = W_c - W_{bp}$, all in eV, slope parameters $S_X = \partial\Phi^{hom}_{Bn}/\partial(X_m - X_s)$ in eV/Miedema unit and electronegativities X_s in Miedema units.

	W_g	I	χ_s	Φ^p_{bp}	Φ^n_{bp}	S_X	X_s
Si	1.12	5.3[a]	4.18	0.30[b]	0.80[c]	0.10[c]	4.70
Ge	0.66	4.7[a]	4.09	0.08[d]	0.59[e]	0.04[e]	4.75
4*H*-SiC	3.26	…	2.54	1.59[f]	1.66[g]	0.21[g]	5.40
6*H*-SiC	3.02	5.8[a]	2.78	1.55[f]	1.35[f]	0.21[f]	5.40
GaN	3.39	6.7[a]	3.31	2.34[b]	1.12[h]	0.27[h]	5.36
GaAs	1.42	5.48[a]	4.06	0.68[d]	0.90[i]	0.08[i]	4.44
ZnO	3.37	7.82[a]	4.45	2.79[b]	…	0.45[j]	5.55
MoS_2	1.20[k]	5.47[l]	4.27	…	0.26[m]	0.12[m]	5.56

[a]See Ref. 36 and references cited therein.
[b]Reference 38.
[c]Reference 40.
[d]Reference 39.
[e]Reference 41.
[f]Reference 6.
[g]From Fig. 4.
[h]From Fig. 3.
[i]Reference 42.
[j]Reference 43.
[k]References 34 and 35.
[l]Reference 37.
[m]From Fig. 5.

IV. METAL-INDUCED INTERFACE BONDS AND INTRINSIC ELECTRIC-DIPOLE LAYERS

As already noted by Mott,[10] the preceding simple *Gedanken* experiment assumes that the metal and the semiconductor "do not influence each other in any way" when the two are placed in contact. However, metal adatoms deposited on clean semiconductor surfaces form chemical bonds with semiconductor surface atoms as indicated by adatom-induced core-level shifts, Δ^{m-s}_{c-l} at the surface atoms of the semiconductors. The experimental chemical shifts Δ^{m-s}_{c-l} of the C(1s), Si(2p), and Ge(3d) core levels exhibit the same linear dependence on the difference $X_m - X_s$ of the electronegativities of the metal and the semiconductor atoms[36] and, hence, prove the partial ionic character of the covalent bonds[44] between the metal adatoms and the semiconductor surface atoms. Calculated charge-density contour plots[45] showed these covalent bonds to persist at metal-semiconductor interfaces and, indeed, the barrier heights of laterally homogeneous Cs-, Na-, Al-, and Ag/n-Si(111) Schottky contacts vary linearly proportional to the Si(2p) core-level shifts induced by the corresponding adatoms on Si(111) surfaces.[46] These experimental findings verify the

existence of *intrinsic* electric-dipoles at metal-semiconductor interfaces. The barrier heights of Schottky contacts are thus composed of a zero-charge-transfer term Φ_{zct} plus an electric-dipole contribution that varies proportional to the core-level shifts Δ_{c-l}^{m-s} and, thereby also, the electronegativity differences $X_m - X_s$. For *n*-type Schottky contacts, one thus obtains

$$\Phi_{Bn} = \Phi_{zct}^{n} + S_{c-l}\Delta_{c-l}^{m-s} = \Phi_{zct}^{n} + S_X(X_S - X_S). \quad (2)$$

The zero-charge-transfer levels $W_{zct} = W_c - \Phi_{zct}^{n}$ have the character of charge-neutrality levels (CNLs).

V. METAL-INDUCED GAP STATES AND INTRINSIC ELECTRIC-DIPOLE LAYERS

The physical counterpart of the metal-induced interface bonds are the metal-induced gap states (MIGSs).[47] They originate from the virtual gap states (ViGSs) of the complex band structure of the semiconductor, i.e., the MIGSs are oscillating and exponentially decaying tails of the metal wave functions across the interface in the energy region where the conduction band of the metal overlaps the band gap of the semiconductor. The evanescent MIGSs are made up of both valence- and conduction-band states of the semiconductor and, therefore, their net charging character changes across the band gap from predominantly donor-like closer to the valence-band top to mostly acceptor-like nearer to the conduction-band edge. The cross-over level where the contributions of both bulk bands are equal is called the branch point W_{bp} of the complex band structure. It has the character of a charge-neutrality level. The *n*-type (*p*-type) branch-point energy $\Phi_{bp}^{n} = W_c - W_{bp}(\Phi_{bp}^{p} = W_{bp} - W_v)$ and the zero-charge-transfer barrier height $\Phi_{zct}^{n}(\Phi_{zct}^{p})$ are identical so that relation (2) may be rewritten as

$$\Phi_{Bn} = \Phi_{bp}^{n} + S_X(X_m - X_s). \quad (3)$$

Since the *n*- and *p*-type branch-point energies add up to the band gap, the *p*-type barrier heights result as

$$\Phi_{Bp} = \Phi_{bp}^{p} - S_X(X_m - X_s). \quad (4)$$

In the following, Miedema's electronegativities[48] will be considered rather than Pauling's[44] since they were derived from properties of metals and their alloys rather than of small molecules. The electronegativities of compounds are the geometrical means of the atomic values of its constituents.[44] The barrier heights Φ_{Bn}^{hom} of intimate, abrupt, and laterally homogeneous diamond, Si,[40] Ge,[41] SiC (see Fig. 4), GaN (see Fig. 3), GaAs,[42] InP,[49] SiO_2,[50] Si_3N_4,[51] and TiO_2 Schottky[6] contacts[52] are all excellently described in relation (3). The linear least-squares fits to such experimental data give the *n*-type branch-point energies Φ_{bp}^{n} and the slope parameters S_X of the particular semiconductors without the input of any additional parameters. Figure 2 shows that the slope parameters S_X of the Schottky contacts mentioned above confirm the dependence

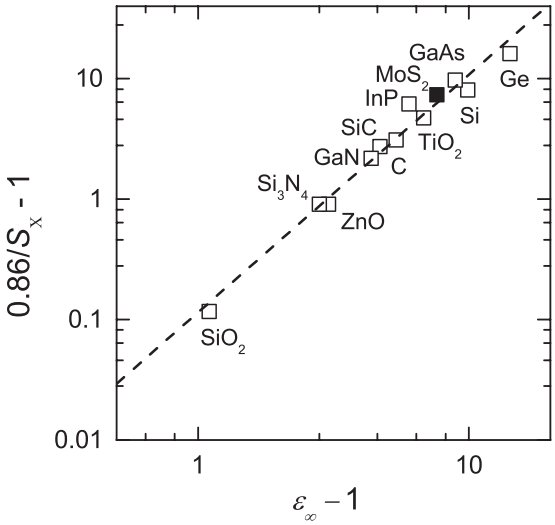

FIG. 2. Experimental slope parameters $S_X = \partial\Phi_{Bn}^{hom}/\partial X_m$ as a function of the optical susceptibility $\varepsilon_\infty - 1$ of the semiconductors. The dashed line is the linear least-squares fit $0.86/S_X - 1 = (0.12 \pm 0.02)(\varepsilon_\infty - 1)^{1.96 \pm 0.10}$ to the data.

$$S_X = \frac{0.86}{0.1(\varepsilon_\infty - 1)^2 + 1}, \quad (5)$$

on the optical dielectric susceptibility $\varepsilon_\infty - 1$ of the semiconductors that was obtained earlier from slope parameters of laterally inhomogeneous Schottky contacts.[53] Relation (5) was also justified by using calculated densities of states and charge decay lengths of the MIGS at their branch points.[54]

VI. BARRIER HEIGHTS OF GRAPHENE SCHOTTKY CONTACTS

The available experimental barrier heights of graphene Schottky contacts behave in exactly the same way as

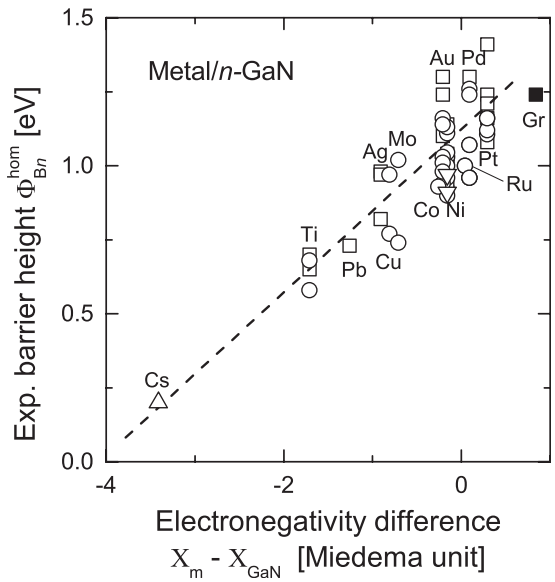

FIG. 3. Experimental barrier heights of laterally homogeneous *n*-GaN Schottky contacts as a function of the electronegativity difference $X_m - X_{GaN}$. Experimental data from Refs. 26, 38, and 55–57. The linear least-squares fit to the data (dashed line) yields the *n*-type branch-point energy $\Phi_{bp}^{n} = (1.12 \pm 0.02)$ [eV] and the slope parameter $S_X = (0.27 \pm 0.02)$ [eV/Miedema unit].

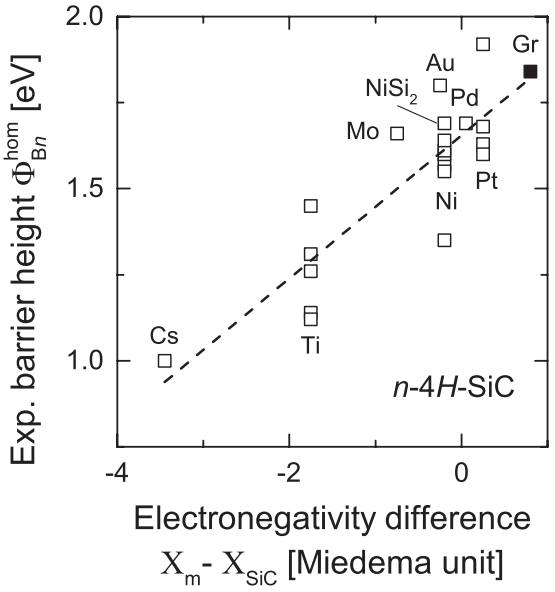

FIG. 4. Experimental barrier heights of laterally homogeneous *n*-4*H*-SiC Schottky contacts as a function of the electronegativity difference $X_m - X_{SiC}$. Experimental data from Refs. 12, 38, and 58–61. The linear least-squares fit to the data (dashed line) yields the *n*-type branch-point energy $\Phi_{bp}^{n} = (1.66 \pm 0.03)$ [eV] and the slope parameter $S_X = (0.21 \pm 0.03)$ [eV/Miedema unit].

"conventional" metal-semiconductor contacts. Figures 3–5 display experimental barrier heights of laterally homogeneous *n*-type GaN, 4*H*-SiC, and MoS_2 Schottky contacts, respectively, not only with "conventional" metals but also with graphene[12,26,29–31] as a function of the respective electronegativity differences. The graphene data points clearly continue the trends set by the "conventional" metals. Most remarkably, MoS_2 behaves the same as the sp^3-bonded semiconductors GaN and 4*H*-SiC although the transition metal

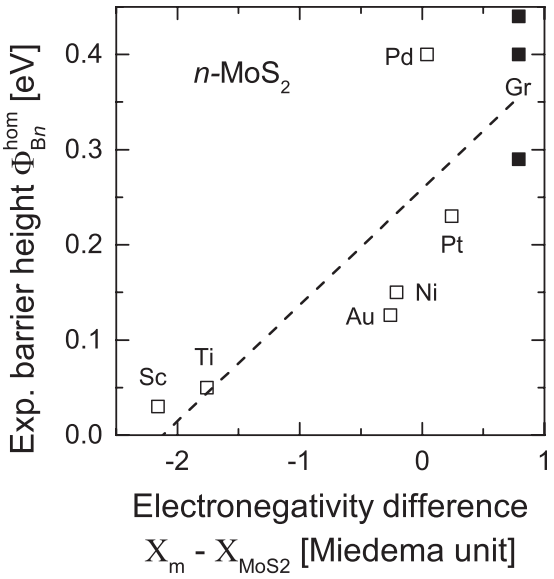

FIG. 5. Experimental barrier heights of laterally homogeneous *n*-MoS_2 Schottky contacts as a function of the electronegativity difference $X_m - X_{MoS2}$. Experimental data from Refs. 29 to31,62, and 63. The linear least-squares fit to the data (dashed line) yields the *n*-type branch-point energy $\Phi_{bp}^{n} = (0.26 \pm 0.03)$ [eV] and the slope parameter $S_X = (0.12 \pm 0.03)$ [eV/Miedema unit].

dichalcogenite has a layered lattice structure that consists of covalently bonded S-Mo-S layers interconnected by weak van der Waals forces. For the MoS_2 Schottky barrier heights plotted in Fig. 5, the linear least-squares fit

$$\Phi_{Bn}^{hom} = (0.26 \pm 0.03) + (0.12 \pm 0.03)(X_m - X_{MoS2}) \quad (6)$$

yields the *n*-type branch-point energy $\Phi_{bp}^{n} = 0.26$ eV and the slope parameters $S_X = 0.12$ eV/Miedema unit. The MoS_2 slope parameter is also included in Fig. 2 ($\varepsilon_\infty = 7$, Ref. 64) and excellently fits in the trend (5) originally found with "conventional" semiconductors.

Guo and Robertson[65] computed the barrier heights of six different *p*-MoS_2 Schottky contacts and obtained a slope parameter $S_X = 0.28$ eV/Miedema unit. More recently, Guo *et al.* (Ref. 66) calculated *p*-type branch point energies of some of the transition-metal dichalcogenites. For MoS_2, they found $\Phi_{bp}^{p} = 0.7$ eV which value gives an *n*-type branch-point energy $\Phi_{bp}^{n} = 0.5$ eV. The calculated partial densities of states at MoS_2 layers away from a Ni/MoS_2 interface revealed the presence of MIGS. Although the branch-point energy Φ_{bp}^{n} and the slope parameter S_X calculated by Robertson and coworkers[65,66] slightly differ, most probably within the margins of experimental and theoretical errors, from the values derived from the experimental data, their theoretical conclusions clearly support the explanation of the MoS_2 Schottky barrier heights by the MIGS-and-electronegativity concept.

The linear dependence of the Schottky barrier heights Φ_{Bn}^{hom} as a function of the electronegativity differences $X_m - X_{semi}$ demonstrates that electric-dipole layers exist at both "conventional" metal-semiconductor interfaces and graphene Schottky contacts. Graphene is more electronegative than the semiconductors so that $Gr^{-\Delta q} - Semi^{+\Delta q}$ interface dipoles will be present. For the most specific case of Gr/MoS_2 contacts, this conclusion is clearly supported by the differential charge densities calculated by Hu *et al.* (Ref. 67). Their results indicate an electron decrease and increase on MoS_2 and the graphene side of such interfaces, respectively. In other words, their calculations yielded, as concluded from the barrier height of Gr/MoS_2 Schottky contacts shown in Fig. 5, a charge transfer from the semiconductor MoS_2 towards the more electronegative graphene. Calculations performed by Chanana and Mahapatra[68] confirmed these conclusions. A similar conclusion was reached by Xia *et al.* (Ref. 69) who calculated the differential charge densities at graphene-arsenene interfaces. They also found a charge transfer from the arsenene to the more electronegative graphene.

VII. GRAPHENE SCHOTTKY CONTACTS AND THE MIGS-AND-ELECTRONEGATIVITY CONCEPT

These findings now suggest that the band-structure lineup at Schottky contacts is determined by the same mechanism irrespective of whether "conventional" metals or graphene are considered, i.e., by the continuum of metal-induced gap states. To prove this conclusion, the experimental barrier heights of the laterally homogeneous Gr Schottky

contacts already shown in Fig. 1 are replotted in Fig. 6 versus the barrier heights

$$\Phi_{Bn}^{MIGS} = \Phi_{bp}^{n}(\text{semi}) + S_X^{semi}(X_{Gr} - X_{semi}), \quad (7)$$

predicted by the MIGS-and-electronegativity concept. The experimental branch-point energies and slope parameters of the respective semiconductors are compiled in Table I. The experimental barrier height of laterally homogeneous Gr/*n*-Ge contacts is larger by 0.3 eV than the Ge band gap and should be re-examined for this reason. The ◆ and ▼ data points will be analyzed in the following paragraphs. The remaining experimental ■ and ● data of the laterally homogeneous Schottky contacts between graphene and the semiconductors *n*-MoS_2, *n*-ZnO, *n*-Si, *n*-GaN, and *n*–4*H*-SiC are excellently explained by the MIGS-and electronegativity concept.

The ◆ barrier heights of Gr/*n*–4*H*-SiC contacts[24] are smaller than the corresponding value predicted by the MIGS concept. These data were obtained with samples, where the 4*H*-SiC surfaces were hydrogenated prior to the transfer of the CVD-grown graphene layer. With hydrogenated Si Schottky contacts, a lowering of the barrier height was also observed[70] and explained by an interface layer of $H^{-\Delta q}$-$Si^{+\Delta q}$ dipoles.[71] Extrinsic dipole layers might thus be responsible for the barrier-height lowering of these Gr/*n*–4*H*-SiC:H contacts.

The conclusion that the MIGS-and-electronegativity concept explains the barrier heights of graphene Schottky contacts is further supported by the experimental data obtained with such contacts that were fabricated on *n*- and *p*-type semiconductor substrates in the exact same manner. Experimental barrier heights of such pairs of graphene Schottky contacts[21,22,27] are compiled in Table II. Figure 7 displays these data as a function of the respective *n*- and *p*-type MIGS barrier heights, (7) and

$$\Phi_{Bp}^{MIGS} = \Phi_{bp}^{p}(\text{semi}) - S_X^{semi}(X_{Gr} - X_{semi}), \quad (8)$$

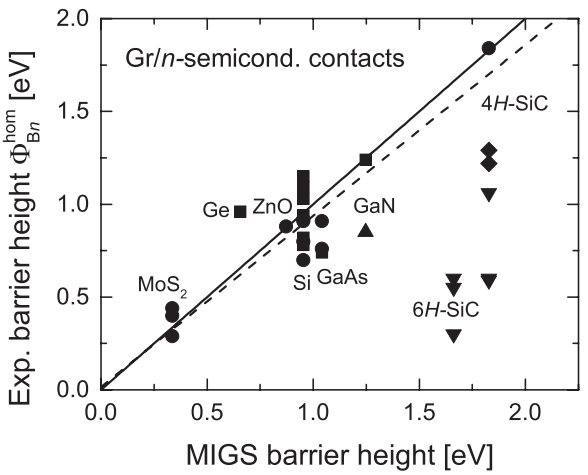

FIG. 6. Experimental barrier heights of laterally homogeneous Gr Schottky contacts as a function of the respective barrier heights predicted by the MIGS concept (6). Same experimental data are plotted as in Fig. 1. The dashed line is the linear least-squares fit to the data.

TABLE II. Barrier heights Φ_{Bn}^{hom} and Φ_{Bp}^{hom} of graphene Schottky contacts that were fabricated on *n*- and *p*-type semiconductor substrates, respectively, in each particular case in the exact same manner and band gaps W_g of the semiconductors. All values are given in eV.

	Φ_{Bp}^{hom}	Φ_{Bn}^{hom}	$\Phi_{Bp}^{hom} + \Phi_{Bn}^{hom}$	W_g
GaN	2.50[a]	0.85[a]	3.35	3.37
4*H*-SiC	2.58[b]	0.59[b]	3.17	3.26
6*H*-SiC	2.32[c]	0.55[c]	2.87	3.02
6*H*-SiC	2.7[b]	0.30[b]	3.00	3.02

[a]Reference 27.
[b]Reference 22.
[c]Reference 21.

respectively. The experimental branch-point energies and slope parameters of the respective semiconductors are compiled in Table I. Table II shows that, within the margins of experimental error, the *p*- and *n*-type barrier heights add up to the band gaps of the particular semiconductors. This finding already indicates that possible *extrinsic* dipole contributions at these interfaces are of identical size on both *n*- and *p*-type contacts. Figure 7 verifies that the barrier heights of the *n*- and *p*-type contact pairs prepared in the exact same manner are indeed lowered and increased by identical amounts, respectively, with regard to values predicted by the MIGS-and-electronegativity concept, namely, by 0.37 eV for GaN,[27] by 1.25 eV for 4*H*-SiC,[22] and by 0.95 and 1.25 eV for 6*H*-SiC contacts (Refs. 21 and 22, respectively.). This behavior is easily explained by the presence of identical extrinsic electric-dipole layers at the interfaces produced in the exact same manner between graphene and the *n*- and *p*-type semiconductor substrates. These extrinsic interface dipoles are typical of the different fabrication methods used.

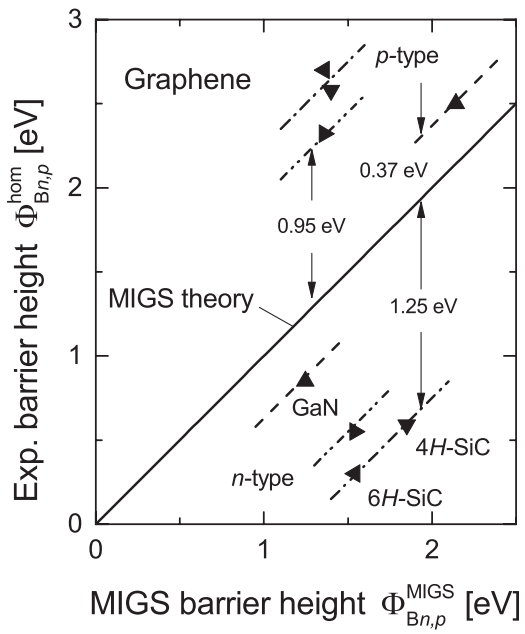

FIG. 7. Experimental barrier heights of laterally homogeneous Gr/GaN, Gr/4*H*-SiC and Gr/6*H*-SiC Schottky contacts fabricated in each case in the exact same manner on samples doped *n*- and *p*-type as a function of the of the respective barrier heights predicted by the MIGS concept (6) and (8), respectively. Experimental data from Refs. 21, 22, and 27.

The differing offsets of 0.95 and 1.25 eV found with Gr/6*H*-SiC contacts by Rheshanov *et al.* (Ref. 22) and Seyller *et al.*,[21] respectively, and the identical offsets of 1.25 eV reported by Rheshanov *et al.* (Ref. 22) for their Gr/4*H*-SiC and Gr/6*H*-SiC contacts directly evidence this conclusion. In this context, it has to be mentioned that Sonde *et al.* (Ref. 72) already discussed the influence of "buffer layers" at the interfaces between graphene fabricated by surface decomposition and the *n*–4*H*-SiC substrates used in their studies. The experimental barrier heights plotted in Fig. 7 thus confirm the conclusion reached above that the MIGS-and-electronegativity concept unambiguously explains the barrier heights of *intimate* and laterally homogeneous Gr Schottky contacts.

These argumentations are also supported by experimental results reported by First *et al.* (Ref. 73) who produced Gr/4*H*-SiC(0001) structures by surface decomposition and examined their electronic structure by using angular-resolved photoemission spectroscopy (ARPES). They found the Fermi level by 0.45 V above the Dirac point where the π and π^* bands of graphene meet, i.e., they observed an accumulation of negative charge on the graphene layer grown on 4*H*-SiC(0001). This finding agrees with the presence of $Gr^{-\Delta q} - SiC^{+\Delta q}$ interface dipoles concluded above from the analysis of the Gr/*n*–4*H*-SiC Schottky contacts.

VIII. CONCLUSIONS

There is one problem left, namely, the nature of the *intrinsic* electronic dipole layer at Gr-semiconductor contacts. The partial ionic character of the covalent bonds between "conventional" metal and "conventional" semiconductor interface atoms, indicated by the chemical core-level shifts of the semiconductor atoms, easily explains the intrinsic dipole layer at such Schottky contacts. However, it is consensus that the graphene-semiconductor bonds are of van der Waals type but not covalent. Nevertheless, theoretical studies yielded a charge transfer across van der Waals-bonded Gr-MoS_2 (Refs. 67 and 68) as well as graphene-arsenene[69] interfaces. In the MIGS-and-electronegativity concept, the calculated electron decrease and increase on the MoS_2 and the graphene side of Gr-MoS_2 contacts, respectively,[67,68] are easily assigned to exponentially decaying tails of the graphene wave functions across the interface in the energy region where the π-π^* bands of the graphene overlap the MoS_2 band gap and to a transfer of negative charge to the more electronegative graphene. This explanation is further supported by the observation that the slope parameter S_X of the *n*-MoS_2 Schottky contacts is excellently described by the semi-empirical rule (5) and, hence, physically explained by the density of states and the charge decay length of the MIGS of the semiconductor MoS_2 at their branch point.

The preceding arguments are not specific to Gr/MoS_2 interfaces but can be applied to all other Gr/semiconductor Schottky contacts. The barrier heights of graphene Schottky contacts are thus explained by the wave-function tails of graphene across the interface in the energy range, where the π-π^* bands of the graphene layer overlap the band gap of the semiconductor. Hence, the barrier heights of "conventional" metal-semiconductor contacts and of graphene Schottky contacts are consistently explained by the MIGS-and-electronegativity concept.

[1]P. R. Wallace, Phys. Rev. **71**, 622 (1947).
[2]S. Reich, J. Maultzsch, and C. Thomsen, Phys. Rev. B **66**, 035412 (2002).
[3]A. Bostwick, T. Ohta, J. L. McChesney, K. V. Emtsev, T. Seyller, K. Horn, and E. Rotenberg, New J. Phys. **9**, 385 (2007).
[4]K. S. Novoselov, V. I. Falko, L. Colombo, P. R. Gellert, M. G. Schwab, and K. Kim, Nature **490**, 192 (2012).
[5]A. K. Geim and K. S. Novoselov, Nat. Mater. **6**, 183 (2007).
[6]W. Mönch, *Electronic Properties of Semiconductor Interfaces* (Springer, Berlin, 2004).
[7]J. L. Freeouf, T. N. Jackson, S. E. Laux, and J. M. Woodall, Appl. Phys. Lett. **40**, 634 (1982).
[8]J. H. Werner and H. H. Güttler, J. Appl. Phys. **69**, 1522 (1991).
[9]R. Schmitsdorf, T. U. Kampen, and W. Mönch, Surf. Sci. **324**, 249 (1995).
[10]N. F. Mott, Proc. Cambridge Philos. Soc. **34**, 568 (1938).
[11]W. Schottky, Phys. Z. **41**, 570 (1940).
[12]S. Tongay, T. Schumann, and A. F. Hebard, Appl. Phys. Lett. **95**, 222103 (2009).
[13]X. Miao, S. Tongay, M. K. Petterson, K. Berke, A. G. Rinzler, B. R. Appleton, and A. F. Hebard, Nano Lett. **12**, 2745 (2012).
[14]S. Tongay, M. Lemaitre, X. Miao, B. Gila, B. R. Appleton, and A. F. Hebard, Phys. Rev. X **2**, 011002 (2012).
[15]C. Yim, N. McEvoy, and G. S. Duesberg, Appl. Phys. Lett. **103**, 193106 (2013).
[16]Y.-J. Lin and J.-J. Zeng, Appl. Surf. Sci. **322**, 225 (2014).
[17]S. Parui, R. Ruiter, P. J. Zomer, M. Wojtaszek, B. J. van Wees, and T. Banerjee, J. Appl. Phys. **116**, 244505 (2014).
[18]D. Tomer, S. Rajput, L. J. Hudy, C. H. Li, and L. Li, Nanotechnology **26**, 215702 (2015).
[19]S. Riazimehr, A. Bablich, D. Schneider, S. Kataria, V. Passi, C. Yim, G. S. Duesberg, and M. C. Lemme, Solid-State Electron. **115**, 207 (2016); private communication (02.03.2016).
[20]M. Zhu, X. Li, X. Li, X. Zang, Z. Zhen, D. Xie, Y. Fang, and H. Zhu, J. Appl. Phys. **119**, 124303 (2016).
[21]Th. Seyller, K. V. Emtsev, F. Speck, K.-Y. Gao, and L. Ley, Appl. Phys. Lett. **88**, 242103 (2006).
[22]S. A. Reshanov, K. V. Emtsev, F. Speck, K.-Y. Gao, T. K. Seyller, G. Pensl, and L. Ley, Phys. Status Solidi B **245**, 1369 (2008).
[23]S. Shivaraman, L. H. Herman, F. Rana, J. Park, and M. G. Spencer, Appl. Phys. Lett. **100**, 183112 (2012).
[24]D. Tomer, S. Rajput, L. J. Hudy, C. H. Li, and L. Li, Appl. Phys. Lett. **105**, 021607 (2014).
[25]Z. Khurelbaatar, Y.-H. Kil, K.-H. Shim, H. Cho, M.-J. Kim, Y.-T. Kim, and C.-J. Choi, J. Semicond. Technol. Sci. **15**, 7 (2015).
[26]R. S. Kim, T. H. Seo, M. J. Kim, K. M. Song, E.-K. Suh, and H. Kim, Nano Res. **8**, 1327 (2015).
[27]C.-L. Tsai, Y.-J. Lin, and J.-H. Lin, J. Mater. Sci. Mater. Electron. **26**, 3052 (2015).
[28]R. Yatskiv, J. Grym, K. Zdansky, and K. Piksova, Carbon **50**, 3928 (2012).
[29]S. Larentis, J. R. Tolsma, B. Fallahazad, D. C. Dillen, K. Kim, A. H. MacDonald, and E. Tutuc, Nano Lett. **14**, 2039 (2014).
[30]Y.-F. Lin, W. Li, S.-L. Li, Y. Xu, A. Aparecido-Ferreira, K. Komatsu, H. Sun, S. Nakaharai, and K. Tsukagoshi, Nanoscale **6**, 795 (2014).
[31]H. Tian, Z. Tan, C. Wu, X. Wang, M. A. Mohammad, D. Xie, Y. Yang, J. Wang, L.-J. Li, J. Xu, and T.-L. Ren, Sci. Rep. **4**, 5951 (2014).
[32]Y.-J. Yu, Y. Zhao, S. Ryu, L. E. Brus, K. S. Kim, and P. Kim, Nano Lett. **9**, 3430 (2009).
[33]R. Yan, Q. Zhang, W. Li, I. Calizo, T. Shen, C. A. Richter, A. R. Hight-Walker, X. Liang, A. Seabaugh, D. Jena, H. G. Xing, D. J. Gundlach, and N. V. Nguyen, Appl. Phys. Lett. **101**, 022105 (2012).
[34]K. K. Kam and B. A. Parkinson, J. Phys. Chem. **86**, 463 (1982).
[35]E. Fortin and W. M. Sears, J. Phys. Chem. Solids **43**, 881 (1982).
[36]W. Mönch, *Semiconductor Surfaces and Interfaces*, 3rd ed. (Springer, Berlin, 2001).
[37]R. Schlaf, O. Lang, C. Pettenkofer, and W. Jaegermann, J. Appl. Phys. **85**, 2732 (1999).
[38]W. Mönch, J. Appl. Phys. **109**, 113724 (2011).
[39]W. Mönch (unpublished).
[40]W. Mönch, J. Vac. Sci. Technol., B **17**, 1867 (1999).

[41]W. Mönch, J. Appl. Phys. **111**, 073706 (2012).
[42]W. Mönch, "Electronic properties of semiconductor interfaces," in *Handbook of Electronic and Photonic Materials*, 2nd ed. (Springer, Berlin, 2016).
[43]M. W. Allen and S. M. Durbin, Phys. Rev. B **82**, 165310 (2010).
[44]L. N. Pauling, *The Nature of the Chemical Bond* (Cornell University, Ithaca, NY, 1939).
[45]S. B. Zhang, M. L. Cohen, and S. G. Louie, Phys. Rev. B **34**, 768 (1986).
[46]W. Mönch, Mater. Sci. Semicond. Process. **28**, 2 (2014).
[47]V. Heine, Phys. Rev.**138**, A1689 (1965).
[48]A. R. Miedema, P. F. de Châtel, and F. R. de Boer, Physica B **100**, 1 (1980).
[49]W. Mönch, Appl. Phys. Lett. **93**, 172118 (2008).
[50]W. Mönch, Appl. Phys. Lett. **91**, 042117 (2007).
[51]Y.-C. Yeo, T.-J. King, and C. Hu, J. Appl. Phys. **92**, 7266 (2002).
[52]W. Mönch, J. Appl. Phys. **107**, 013706 (2010).
[53]W. Mönch, Phys. Rev. Lett. **58**, 1260 (1987).
[54]W. Mönch, Appl. Surf. Sci. **92**, 367 (1996).
[55]M. S. P. Reddy, A. A. Kumar, and V. R. Reddy, Thin Solid Films **519**, 3844 (2011).
[56]N. N. K. Reddy and V. R. Reddy, Bull. Mater. Sci. **35**, 53 (2012).
[57]B. Roul, T. N. Bhat, M. Kumar, M. K. Rajpalke, A. T. Kalghatgi, and S. B. Krupanidhi, Phys. Status Solidi A **209**, 1575 (2012).
[58]B. J. Skromme, E. Luckowski, K. Moore, M. Bhatanagar, C. E. Weitzel, T. Gehoski, and D. Ganser, J. Electron. Mater. **29**, 376 (2000).
[59]F. Roccaforte, F. La Via, V. Raineri, R. Pierobon, and E. Zanoni, J. Appl. Phys. **93**, 9137 (2003).
[60]D. J. Ewing, L. M. Porter, Q. Wahab, X. Ma, T. S. Sudharshan, S. Tumakha, M. Gao, and L. J. Brillson, J. Appl. Phys. **101**, 114514 (2007).
[61]F. Giannazzo, F. Roccaforte, and V. Raineri, Microelectron. Eng. **84**, 450 (2007).
[62]S. Das, H.-Y. Chen, A. V. Penumatcha, and J. Appenzeller, Nano Lett. **13**, 100 (2013).
[63]N. Kaushik, A. Nipane, F. Basheer, S. Dubey, S. Grover, M. M. Deshmukh, and S. Lodha, Appl. Phys. Lett. **105**, 113505 (2014).
[64]R. F. Frindt and A. D. Yoffe, Proc. Roy. Soc. (London) A **273**, 69 (1963).
[65]Y. Guo and J. Robertson, Microelectron. Eng. **147**, 184 (2015).
[66]Y. Guo, D. Liu, and J. Robertson, ACS Appl. Mater. Interfaces **7**, 25709 (2015).
[67]W. Hu, T. Wang, R. Zhang, and J. Yang, J. Mater. Chem. C **4**, 1776 (2016).
[68]A. Chanana and S. Mahapatra, J. Appl. Phys. **119**, 014303 (2016).
[69]C. Xia, B. Xue, T. Wang, Y. Peng, and Y. Jia, Appl. Phys. Lett. **107**, 193107 (2015).
[70]T. U. Kampen and W. Mönch, Surf. Sci. **331–333**, 490 (1995).
[71]W. Mönch, Europhys. Lett. **27**, 479 (1994).
[72]S. Sonde, F. Giannazzo, V. Raineri, R. Yakimova, J.-R. Huntzinger, A. Tiberj, and J. Camassel, Phys. Rev. B **80**, 241406 (2009).
[73]P. N. First, W. A. de Heer, T. Seyller, C. Berger, J. A. Stroscio, and J.-S. Moon, MRS Bull. **35**, 296 (2010).